Stress Calculation for the Sandia 34–Meter Wind Turbine Using the Local Circulation Method and Turbulent Wind

Bernard Massé and Henri Pastorel

IREQ Institut de Recherche d'Hydro–Québec, Québec, Canada

ABSTRACT

Stress calculation for wind turbine blades is an important task for the manufacturers of wind turbines. A good prediction of stress level is required to evaluate the fatigue life of the rotor. Design of critical blade joints is based on such calculations. Aerodynamic loads are responsible for much of the stress level, and atmospheric turbulence has been identified as an important factor in estimating fatigue damage.

This paper describes a stress estimation procedure and its application for the Sandia DOE 34–meter wind turbine. The procedure uses the computer code developed at IREQ (MCL) for aerodynamic loads calculation including atmospheric turbulence.

Aerodynamic loads are decomposed into modal components and applied to the structure using the general purpose finite element program MSC/NASTRAN. The stress distributions as functions of frequency are extracted for critical locations on the blade. Stress distributions are calculated for the first five harmonics of the rotational speed and for off–harmonic frequencies. Comparison with measured data is good but a few questions about damping factors and aeroelastic phenomena are raised.

INTRODUCTION

Loads on the blades of vertical axis wind turbines, including those of the Darrieus type, are cyclic due to rotation of the blade upwind and downwind. This constantly changes the orientation of the blade relative to the wind, leading to changes in angle of attack and aerodynamic loads. As this effect is related to the rotation of the rotor, the frequencies contained in the load signal occur at integer multiples of the rotational frequency. Atmospheric turbulence adds stochastic components to cyclic loads, introducing energy between each per revolution cyclic frequency. Experimental stress measurements show the cyclic nature of the response as well as the stochastic effect on the structure.

Several studies were conducted in the past to model atmospheric turbulence on other structures than wind turbines and NASA published a good handbook related to wind turbines in 1979 [2.] Models for spectral densities and spatial coherence in a neutral atmosphere are already well defined. The use of turbulence models to calculate unsteady aerodynamic loads on wind turbine blades is recent but justified by experimental observations that turbulence has a significant impact on the fatigue life of the structure. This impact is more relevant for a large-size rotor as low-frequency content of turbulence is prone to excite low-vibration modes of the structure.

Sandia National Laboratories [3.] was the first to introduce turbulence models for load and stress calculation on Darrieus rotor blades. Indal Technologies [4.] has used Sandia models to estimate stresses on the blades of their 6400-500Kw wind machine. Both used the double-multiple streamtube aerodynamic model to calculate aerodynamic loads. Recently, IREQ [5.] introduced the local circulation model for aerodynamic load calculation. Comparisons have been made with experimental stress measurements by different authors. Agreement between measured and predicted stress data is not complete in all cases published to date, and many aspects are being questioned. Differences between results from various calculation methods can be produced by different aerodynamic model, the way the dynamic stall is introduced, assumptions about the behavior of the turbulent flow field passing through the rotor, the time-domain or the frequency-domain approach used in structural codes, the random or deterministic solution used and other differences in computation methods. Aerodynamic models used to estimate stochastic loads based on the double-multiple streamtube codes, as used by Sandia and Indal, are quasi-static and probably not completely suitable when turbulence is introduced.

The objective of this work was to investigate an alternative way to calculate stresses on the 34-meter Sandia/DOE Test Bed wind turbine with atmospheric turbulence included. Turbulence is introduced using Veers' [3.] model.The unsteady local circulation model of IREQ (MCL) [1.] was used to calculate the aerodynamic loads, and an IREQ structural code was used to determine the turbine stuctural response.

UNSTEADY AERODYNAMIC LOADS WITH TURBULENCE

Aerodynamic codes based on momentum theory miss important effects of unsteady flow for the following reasons:

- wake effects are not considered because no wake model is used.
- wake crossing by the blades is not considered.
- streamtubes are assumed independent, with no interaction between the tubes.
- unsteady effects, like turbulence, are considered as a succession of static solutions.

The unsteady aerodynamic code, MCL, which IREQ developed, does not have those limitations. The code uses a time-marching method so that the vorticity shed by the rotor blades is transported downstream by the prescribed wake. The wake downstream from the rotor contains the vorticity shed previously by the blades and induces velocities back to the blades a few moments later. This "delay" is not considered in streamtube models. As a first step, turbulence was introduced in MCL as described in the following section.

Interfacing the turbulence model with the MCL code

For the present project, the Kaïmal spectrum as suggested by Frost [2.] was used. If f is the frequency, V is the wind speed at 10 meters from the ground, h is the height, Z_0 is the surface roughness coefficient, and C_1 and C_2 are constants which differ for longitudinal and lateral directions, the spectral density is expressed as follows:

$$S(f) = \frac{C_1 V \; h \left[\ln\left(\frac{10}{Z_0}+1\right) \ln\left(\frac{h}{Z_0}+1\right)\right]^{-1}}{1 + C_2 \left[\frac{h f \ln(10/Z_0 + 1)}{V \ln(h/Z_0 + 1)}\right]^{\frac{5}{3}}}$$

The values used for C_1 and C_2 are the same suggested by Frost and used by Veers and Malcolm, as no better values were known from test site atmospheric data.

Turbulence is calculated using the method published by Veers [3.] and described by Malcolm in reference [4.]. This method consists of generating turbulence time series at an array of points in space upstream of the rotor. For each of the points in the array, the time series represents longitudinal and lateral perturbations about a mean value. Details of the time series generation are not given in this paper; they are described by Veers.

We assume that the perturbations travel downstream with the general flow, as influenced by the wake-induced velocities. Inside the rotor, a linear variation is assumed, as illustrated in Figure 1.

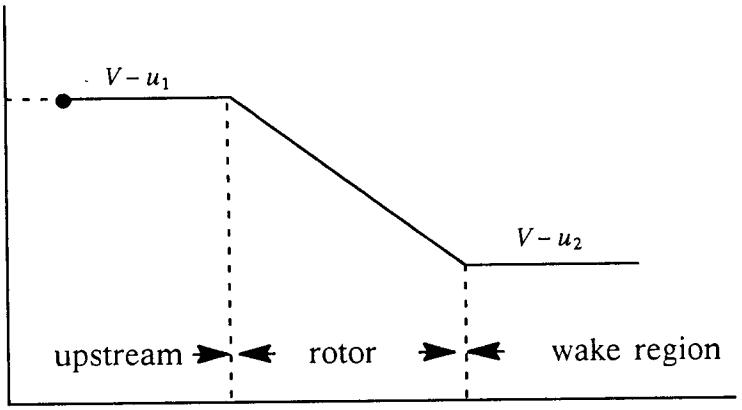

Figure 1: Wind velocity through the rotor

The assumption that the perturbations are passed through the rotor with a velocity influenced by the wake is not straightforward. Velocities induced by the wake must be known inside the rotor to calculate the speed of the perturbations. The perturbations influence the general flow and the induced velocities required to locate these perturbations. One way to resolve the problem is to suppose that the perturbations move with the flow's velocity without influence from induced velocities from the wake. Since the induced velocities are an important part of the main stream flow, this assumption is not acceptable.

A better assumption was made. MCL uses a closed form solution for the wake-induced velocities to calculate initial values to start the simulation. It has been shown that, compared to the unsteady induced velocities, this estimation is quite good [1.]. The assumption is that the induced velocities obtained from the closed form solution, which are as accurate as the solution from the double-multiple streamtube models, are used to calculate the positions of perturbations in the flow field. The velocity upstream of the rotor is the velocity of the uniform flow minus the velocity induced by the wake at the upstream crossing of the rotor blade trajectory. Downstream, the uniform flow field is

reduced by the value of the induced velocity of the downstream rotor azimuthal crossing. Inside the rotor, a linear estimation between the two values is used.

Figure 2 shows in a schematic view the displacement of the perturbations within the rotor. Each perturbation is moved downstream along a straight line with a velocity equal the sum of the free-stream velocity and the induced velocities. In this figure the rotational plane is shown for two different heights, close to the top of the rotor and close to the equator. The spacing between transverse lines shows that wind speed is larger near the top as compared to the equator. This is the effect of wind shear. The curvature of those lines is an indication of the differences in transport velocity between the center of the rotor and the edges. The flow is largely retarded in the center and almost undisturbed at the edges. This retardation is also more severe at the equator than near the top. As the blades cross this field of perturbations, the local velocity of the flow field is calculated for each blade at each time step.

The perturbations as "seen" by the blades must be evaluated at different heights and different azimuthal positions. The locations at which local velocities, including perturbations, are required do not correspond exactly to the locations where perturbations are known. Some interpolation is needed to estimate all the values required, because it is not yet possible to calculate the perturbations at every point used in the aerodynamic model. To avoid interpolation between time series of stochastic nature, along the height of the rotor, the time series closest to the desired location is used. The time series close to the equator influences a certain zone close to the equator, and so on for different heights.

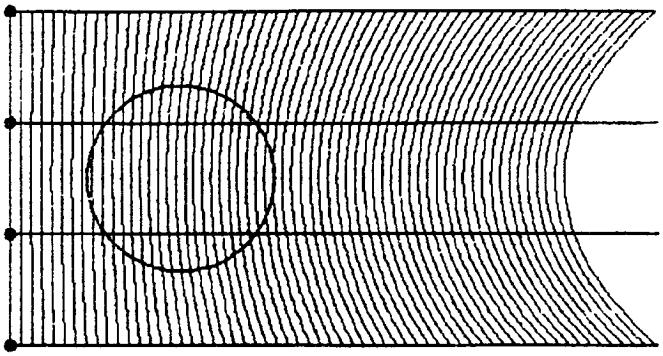

section near top

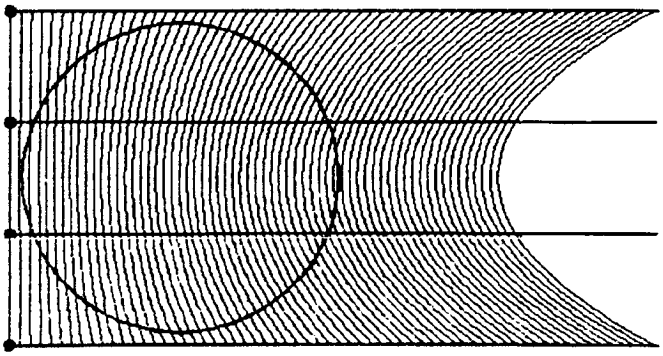

section at equator

Figure 2: Schematic view of the displacement of perturbations through the rotor

In the rotational plane, the blade position is calculated, and the closest series is used for the perturbations. This is done again to avoid interpolation between two series. The only interpolation used is within the same time series, along the wind direction, to estimate the longitudinal and transverse perturbations between two points on a fine grid (see Figure 2).

Performance estimation with MCL

Performance for the Sandia National Laboratories (SNL) 34-meter turbine at 28 and 34 rpm were estimated using MCL. The results are presented in Figure 3, where MCL is compared to SLICEIT from SNL and experimental data from the 34-meter Test Bed. As shown in Figure 3, the results obtained with MCL differ from those calculated with SLICEIT, which is a double-multiple streamtube code using the same airfoil data and a very similar dynamic stall model. The calculation with MCL agrees well with measured data.

The double-multiple streamtube model underestimates power at both rotational speeds, the under-prediction being more severe at 34 rpm. For low winds, both codes overestimate the performance at both rotational turbine speeds, the overestimation being less severe for MCL. This behavior indicates that rotor drag is larger than that estimated from airfoil data. This seems to be confirmed by Berg [6. and 7.].

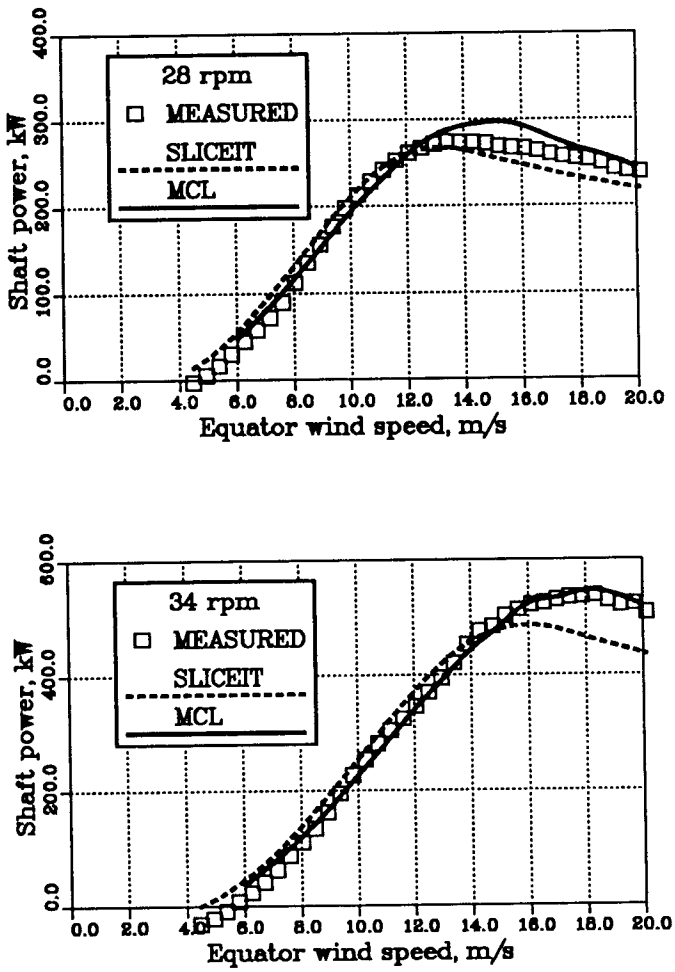

Figure 3: Performance of Sandia's 34-m Test Bed

Aerodynamic loads with turbulence

Unsteady aerodynamic code MCL is used for a turbulent flow field to estimate the unsteady aerodynamic loads applied at different locations along the blades. Turbulence, being considered as local velocity perturbations, is introduced in the load calculation as a modification of the angle of attack and the relative wind velocity. The corresponding changes of vorticity in the wake are kept from one time step to the other, and introduce a delay in the induced effects.

Direct validation of aerodynamic loads is not feasible. The response of the rotor under the action of such aerodynamic loading is the only means of evaluation. If computed stresses compare with measured values, one can assumed that aerodynamic input is valid. The following sections describe how calculated aerodynamic loads are used to calculate unsteady stresses for critical blade locations.

INTERFACING WITH MSC/NASTRAN

To introduce unsteady aerodynamic loads as input for MSC/NASTRAN, the time series are first transformed into the frequency domain and are then used for the solution at each frequency. This type of interface allows the user to select an arbitrary number of revolutions in aerodynamic simulation and it still gives the possibility of solving for a constant number of frequencies in the structural calculation. A Fourier transform of each load time series is performed for the frequency range of interest. The loads are then introduced in MSC/NASTRAN on each node of the blades.

Aerodynamic loads on structural nodes

A computer program has been developed to read the node coordinates where aerodynamic loads are applied and to convert from aerodynamic elements to structural elements. MCL utilizes 16 nodes, as shown in Figure 4, which are more concentrated close to the equator, the loads being larger in this area. For structural calculation, the blade is modeled using 44 nodes concentrated close to the roots and the blade–blade joints.

The aerodynamic loads at the structural nodes used by MSC/NASTRAN are obtained using cubic spline interpolation between loads calculated by MCL at aerodynamic nodes. This is done at each frequency of interest. The aerodynamic input consists of real and imaginary components of the normal and tangential loads for each aerodynamic node for the two blades. The translation program converts the loads to structural nodes in the system of coordinates used in MSC/NASTRAN.

Interpolation to determine loads between the aerodynamic nodes is not the ideal situation because of stochastic content of the loads, but it allows the use of more complex aerodynamic simulations. A simulation for each structural node would require a large amount of computer time.

EIGENFREQUENCIES AND MODE SHAPES

A structural model of the SNL 34–meter wind turbine was obtained from Sandia. The first task was to verify the model by calculating the Campbell diagram (fan plot). The procedure used was developed at IREQ and, was already checked, against Sandia's computer code FEVD using the Magdalen Island wind turbine [8.].

Work is done in two parts. First, the non–linear stiffness matrix, the Corriolis and the softening matrices are calculated using solution 64 of MSC/NASTRAN, modified by a DMAP code developed at IREQ. Then, modes and frequencies are evaluated using solution 70 of MSC/NASTRAN assuming that the non–linear stiffness matrix is proportional to the square of the rotational velocity. This work requires a DMAP code to modify solution 70.

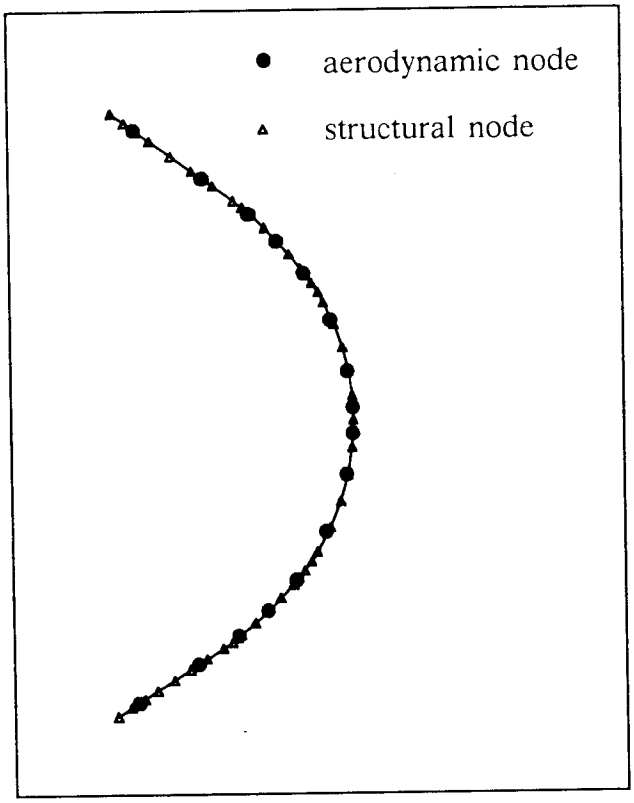

Figure 4: Aerodynamic and structural nodes

Table 1: Parked frequencies

Mode	IREQ calculated	Sandia calculated	Sandia measured	IREQ deviation	Sandia deviation
1FA	1.05	1.05	1.06	1.0%	1.0%
1FS	1.05	1.05	1.06	1.0%	1.0%
1Pr	1.60	1.56	1.52	5.2%	2.6%
1BE	1.70	1.72	1.81	6.4%	5.2%
2FA	2.05	2.07	2.06	0.7%	0.5%
2FS	2.12	2.14	2.16	1.9%	1.0%
1TI	2.42	2.46	2.50	3.2%	1.6%
1TO	2.55	2.58	2.61	2%	1.2%

Table 1 (legend): Mode Shape Abbreviations	
1FA	First Flatwise Antisymmetric
1FS	First Flatwise Symmetric
1Pr	First Propeller
1BE	First Blade Edgewise
2FA	Second Flatwise Antisymmetric
2FS	Second Flatwise Symmetric
1TI	First Tower In-Plane
1TO	First Tower Out-of-Plane

Parked frequencies

To compute the parked frequencies, the geometric finite element model from Sandia was used. The analysis method used is a Guyan reduction technique followed by a modified Givens solution. All translational degrees of freedom are retained in the Guyan reduction. Table 1 shows a comparison with Sandia's analytical calculation and experimental measurements.

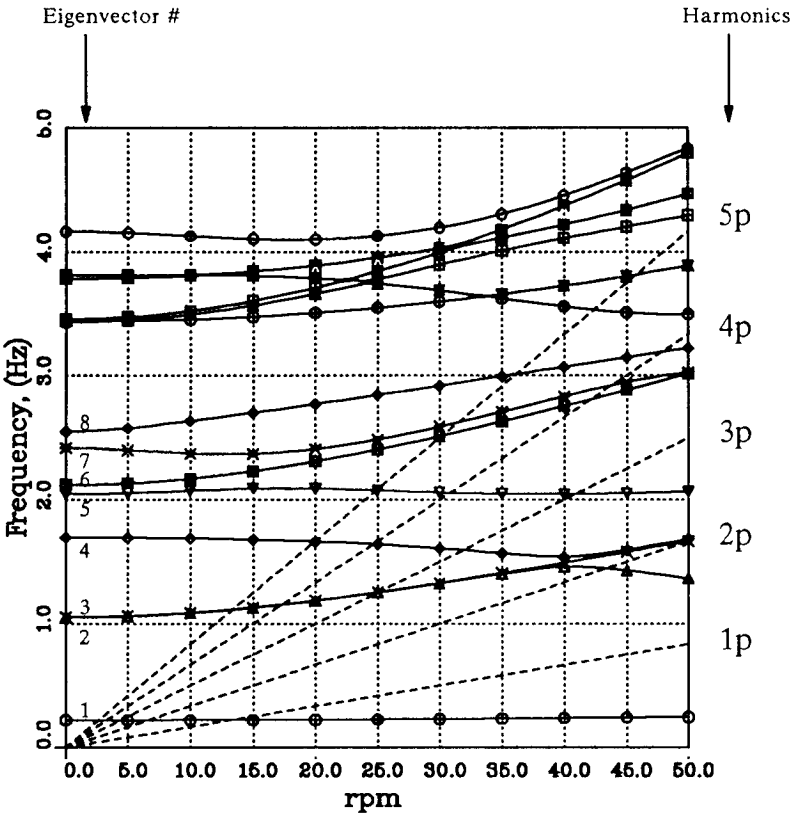

Figure 5: Rotating modal frequencies

Rotating frequencies and eigenvectors

Figure 5 shows the Campbell diagram for the SNL 34-meter turbine, calculated using the approach described above.

Table 2 shows a comparison of the first twelve frequencies computed at Sandia and IREQ at 30 rpm . The results show a maximum deviation of 1% at 4 Hz and confirm that geometric and Coriolis effects are properly introduced.

Table 2: Frequencies and mode shapes at 30 rpm

Complex eigenvectors			Frequencies		
Order	**Real part**	**Imagi-part**	**IREQ**	**Sandia**	**Differ-ence**
1	1PR	-	0.23	0.23	0%
2	1FA	-	1.32	1.31	0.8%
3	1FS	-	1.33	1.32	0.8%
4	1BE, 1TO	1TI, 1FA	1.61	1.61	0%
5	2FA, +1TI	1TO, 1BE	2.06	2.06	0%
6	2FS	3PR	2.51	2.51	0%
7	2FA, -1TI	1TO, 1BE	2.59	2.59	0%
8	1TO, 1BE	1TI, 2FA	2.92	2.92	0%
9	2PR	3FS, 1FS	3.60	3.62	0.6%
10	2BE, -2TO	2TI	3.69	3.69	0%
11	3FA, 2TI	2BE, 2TO	3.90	3.94	1.0%
12	3FS, 2FS	3PR, 2PR	4.00	4.04	1.0%

STRESS CALCULATIONS AND THEIR RESULTS

Stress computation is done directly in MSC/NASTRAN. Aerodynamic loads from MCL are translated in NASTRAN format using an aerodynamic-structure interface code. The first step is done using the modified solution 64 and the second step with solution 71, frequency modal response. The results were obtained with only one simulation per case of turbulence.

Tables 3 and 4 show stress results at the upper root-blade connection, computed at 10% and 30% turbulence levels. Computed stresses are compared at harmonic and off-harmonic frequencies with experimental stresses measured by Sandia on the 34-meter Test Bed.

The effect of increasing turbulence level is a reduction of harmonic stresses (table 3) with the exception of the lead-lag stress at 4P where an increase is observed. Stress reduction is more important at 2P, 3P, 4P and 5P than for 1P. The general tendency of the computations as compared with measured values is to overestimate the stresses, except at 1P where they are underestimated. Flatwise stresses at 2P are well overestimated because of a close resonance condition of the 1FS mode. The 1FS mode is probably highly damped by the aeroelastic damping because of the flatwise motion. However, a reduction from 7.6 MPa

to 4.17 MPa cannot be produced by aeroelastic damping only, a value of 30% of critical damping is required to produce that reduction. The overestimation at 5P, in both flatwise and lead-lag stresses, is due to a near resonance condition for eigenvector 7. At this frequency, the coupling between 2FA, mixed with 1TI, and 1BE mixed with 1TO, induces both lead-lag and flatwise stresses. Aerodynamic damping would reduce the overestimation by damping in-plane modes, but not enough to bring computed values in the range of measured data.

Table 3: Harmonic stresses in MPa at 34 rpm in a 15.6 m/s wind

	10% turb. 2% mod. da. 2% str. da.		30% turb. 2% mod. da. 2% str. da.		Sandia experimental data	
Freq.	**Flat-wise**	**Lead-Lag**	**Flat-wise**	**Lead-Lag**	**Flat-wise**	**Lead-Lag**
1P	1.54	2.51	1.46	2.53	2.20	1.48
2P	7.56	1.20	6.14	0.70	4.17	0.89
3P	2.33	1.40	1.48	0.43	1.51	1.55
4P	1.14	0.48	0.77	0.72	0.86	0.24
5P	2.46	1.29	1.92	0.29	0.40	0.29

Table 4: Off-Harmonic stresses in MPa at 34 rpm in a 15.6 m/s wind

	10% turb. 2% mod. da. 2% str. da.		30% turb. 2% mod. da. 2% str. da.		Sandia experimental data	
Freq.	**Flat-wise**	**Lead-Lag**	**Flat-wise**	**Lead-Lag**	**Flat-wise**	**Lead-Lag**
1.28	2.14	-	6.12	-	1.7	-
1.39	4.00	1.39	8.94	2.70	1.34	0.46
1.51	1.24	-	0.55	-	0.55	-
1.55	-	1.62	-	5.00	-	0.51
1.62	-	1.58	-	3.20	-	1.09
2.04	-	1.00	-	1.46	-	0.94
2.56	0.92	-	2.75	-	0.78	-
2.68	1.55	-	2.70	-	0.46	-

From Table 4, showing *off-harmonic stresses*, it can be seen that stresses are overestimated compared with measured values and strongly correlated with the turbulence level. Turbulence excites resonances that are sensitive to damping. An aeroelastic model would damp flatwise resonances, improving off-harmonic stresses estimation.

Comparison with results from Malcolm [4.]

The results presented in the preceding section show a flatwise stress underestimation at 1P. Malcolm used the "Mode Acceleration Module (MAM)" of MSC/NASTRAN to approximate the effect of high frequency modes neglected in the modal response [4.]. This module was also used in the current work and results are shown in Table 5.

Table 5: Harmonic stresses in MPa at 34 rpm in a 15.6 m/s wind with 10% turbulence using 2% modal damping and 2% structural damping.

	without MAM		with MAM		experimental	
Fre-quency	Flat-wise	Lead-Lag	Flat-wise	Lead-Lag	Flat-wise	Lead-Lag
1P	1.54	2.51	2.70	3.00	2.20	1.48
2P	7.56	1.20	8.05	1.32	4.17	0.89
3P	2.33	1.40	2.18	1.43	1.51	1.55
4P	1.14	0.48	1.17	0.42	0.86	0.24
5P	2.46	1.29	2.46	1.29	0.40	0.29

The high frequency modes approximation modifies 1P and 2P stresses but insures a good numerical stability when the number of modes is increased in the modal response solution. The effect on off-harmonic stresses is negligible.

A comparison with Sandia measured data and Malcolm's predictions, using the TRES4 computer model, [9.] is shown in Figures 6 and 7.

Figure 6 shows a good agreement for flatwise stresses at 10% turbulence. The 2P response is slightly higher in IREQ's model. There is a 1FS response at 1.39 Hz in our results that is not present in Malcolm's calculation due to the aeroelastic damping effect. The 3P response is in better agreement with experimental data in IREQ's model. In the edgewise direction, IREQ's model is closer to experimental data (Figure 7) in the 1.5 - 1.7 Hz range and again 3P response is closer to measured values. This seems to indicate that the phase of 3P aerodynamic excitation from MCL is different as compared to the phase produced from the DMST model. To excite the 1.58 Hz complex eigenvector, the 3P aerodynamic loading must be in phase with the eigenvector. Experimental data do not show such a behavior and IREQ's calculations are in the same direction. The differences between flatwise and edgewise responses when compared to Malcolm's results tend to indicate that aeroelastic damping is responsible for most of the other differences between the two prediction models.

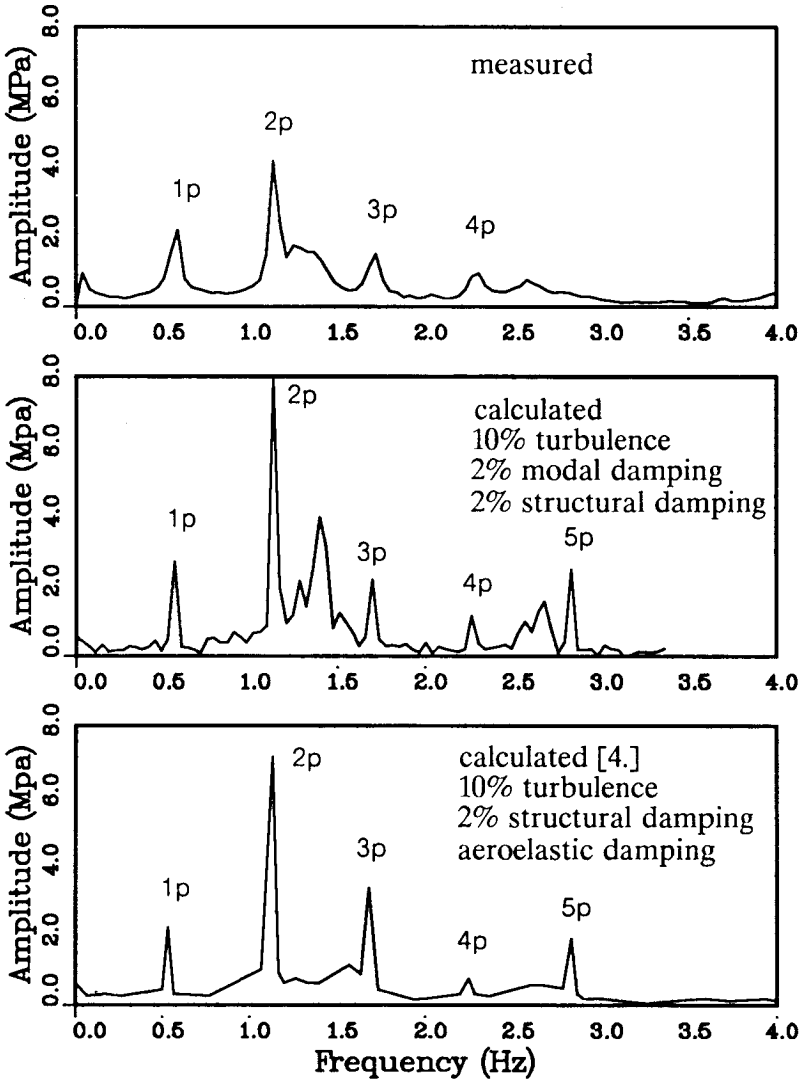

Figure 6: Amplitude spectra of flatwise stress response at 34 rpm, 15.6 m/s wind

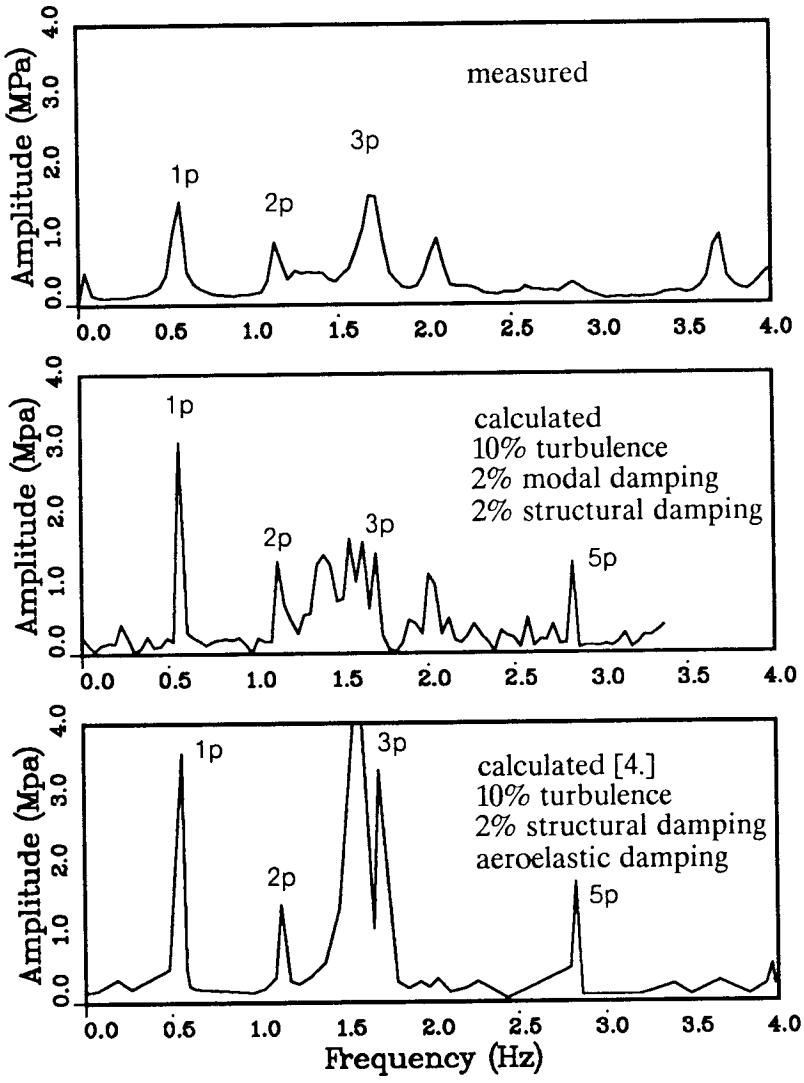

Figure 7: Amplitude spectra of lead-lag stress response at 34 rpm, 15.6 m/s wind

CONCLUSIONS

A new aerodynamic approach was used to evaluate unsteady blade stresses on the Sandia 34-meter wind turbine. Atmospheric turbulence is considered and introduced in the aerodynamic load calculations using the local circulation method code MCL developed at IREQ. Performance data for the Sandia 34-meter Test Bed were obtained at 28 and 34 rpm, and the agreement with experimental data is good. The performance of the Sandia 34-meter machine at 34 rpm is well predicted by MCL over most of the wind speed range, including 15.6 m/s, where the stresses are estimated.

Interface with the structure is done using a computer code to transfer the aerodynamic loads from the aerodynamic blade nodes to structural nodes. Stresses are computed using a modal approach introduced in a MSC/NASTRAN procedure.

The stresses obtained are compared with the measured values in the lead-lag and the flatwise directions at the root of the blade. Results are compared with experimental data using the amplitude spectra. Lead-lag stress predictions compare well with field data and advantageously with Malcolm's results [4.], taking into account the uncertainties related to turbulent flow field, aerodynamic load estimations, structural assumptions and measurement averaging. However, further work is required to see if most of the discrepancies between IREQ and Malcolm models are produced by aeroelastic damping.

REFERENCES

[1.] Massé, B., "Calcul des forces aérodynamiques instationnaires sur les pales d'une turbine d'aérogénérateur à axe vertical", Université de Sherbrooke, Thèse de doctorat, Octobre 1987. (aussi rapport IREQ-RT4111G).

[2.] Frost, W. et al., "Engineering Handbook on the Atmospheric Environmental Guidelines for Use in Wind Turbine Generator Development", NASA Technical paper 1359, December 1979.

[3.] Veers, P. S., "Modeling Stochastic Wind Loads on Vertical Axis Wind Turbines", Sandia Report SAND83-1909, September 1984.

[4.] Malcolm, D., "Vertical Axis Wind Turbine Turbulent Wind Response Model", Final Report Vol 1 & 2, Indal Technologies Inc., February 1987. (Also SAND88-7021, July 1988).

[5.] Massé, B., Pastorel, H. and Heilmann, W., "Nouveau modèle aérodynamique pour le calcul des effets de la turbulence atmosphérique sur les éoliennes Darrieus", Energie, Mines et Ressources Canada, Rapport final, juin 1989. (aussi rapport IREQ-4516, nov. 1989).

[6.] Berg, D., "To Paint or not to Paint-What Price Beauty ? ", Ninth Annual Vertical Axis Wind Turbine Research Seminar, Bushland, Texas, April 4-5, 1989.

[7.] Berg, D., "Test Bed Blade / Blade Joint Fairings", Ninth Annual Vertical Axis Wind Turbine Research Seminar, Bushland, Texas, April 4-5, 1989.

[8.] Pastorel, H., "Méthode simplifiée de calcul des fréquences de résonnance de rotors d'éoliennes à axe vertical", Juin 1984, rapport IREQ-8RT3079G.

[9.] Ashwill, T. D. and Veers, P. S., "Structural Response Measurements and the Predictions for the Sandia 34-meter Test Bed", To be presented at the Ninth ASME Wind Energy Symposium, New Orleans, LA, January 14-17, 1990.